Journal Pre-proof

Potential impacts of future reduced aerosols on internal dynamics characteristics of precipitation based on model simulations over southern China

Yadong Lei, Feng Zhang, Lijuan Miao, Qiu-Run Yu, Mingkeng Duan, Klaus Fraedrich, Zifeng Yu

PII: S0378-4371(19)32119-3
DOI: https://doi.org/10.1016/j.physa.2019.123808
Reference: PHYSA 123808

To appear in: *Physica A*

Received date : 29 July 2019
Revised date : 13 November 2019

Please cite this article as: Y. Lei, F. Zhang, L. Miao et al., Potential impacts of future reduced aerosols on internal dynamics characteristics of precipitation based on model simulations over southern China, *Physica A* (2019), doi: https://doi.org/10.1016/j.physa.2019.123808.

Highlights:

- Precipitation records over southern China exhibit relatively weak long-term correlation characteristics.
- The CESM1 model has the better performance in simulating the internal dynamics characteristics of precipitation series in southern China.
- The future reduced aerosols emissions will contribute to strengthening the long-term correlation of precipitation records in Huai river basin in summer during the late-21st century (2071-2100).

Potential impacts of future reduced aerosols on internal dynamics characteristics of precipitation based on model simulations over southern China

Yadong Lei[a,b], Feng Zhang[a,c*], Lijuan Miao[d], Qiu-Run Yu[a], Mingkeng Duan[a,c], Klaus Fraedrich[e], and Zifeng Yu[f]

[a]*Key Laboratory of Meteorological Disaster, Ministry of Education (KLME)/ Joint International Research Laboratory of Climate and Environment Change (ILCEC)/ Collaborative Innovation Center on Forecast and Evaluation of Meteorological Disaster (CIC-FEMD), Nanjing University of Information Science and Technology, Nanjing, 210044, China*

[b]*Climate Change Research Center, Institute of Atmospheric Physics, Chinese Academy of Sciences, Beijing, 100029, China*

[c]*State Key Laboratory of Severe Weather, Chinese Academy of Meteorological Sciences, Beijing, 100081, China*

[d]*Collaborative Innovation Center on Forecast and Evaluation of Meteorological Disasters, School of Geography Science, Nanjing University of Information Science and Technology, Nanjing, 210044, China*

[e]*Max Planck Institute of Meteorology, Hamburg 20146, Germany*

[f]*Shanghai Typhoon Institute, China Meteorological Administration, Shanghai, 200030, China*

Corresponding author: Feng Zhang (fengzhang@nuist.edu.cn)

Abstract: In this study, the scaling behaviors of precipitation records over southern China are investigated by using the detrended fluctuation analysis (DFA) method. It is found that the precipitation records over southern China exhibit relatively weak long-term correlation characteristics. The scaling exponents in coastal areas are close to 0.6 showing long-term correlation while in inland areas, uncorrelation can be found with the scaling exponents close to 0.5. Based on the long-term correlation characteristics of the observed precipitation records, the performance of Community Earth System Model (CESM1) in simulating precipitation over southern China is evaluated and the results show that the CESM1 has the ability to simulate the internal dynamics characteristics of precipitation series in southern China. As indicated by the DFA results of simulated precipitation data from CESM1, the long-term correlation of precipitation records during the late-21st century (2071-2100) will increase in Huai river basin under the RCP8.5 simulation scenario in summer and decrease in most regions of southern China under both the RCP8.5 and RCP8.5_FixA scenarios in comparison with the present condition (1987-2016). And the differences of scaling exponents of precipitation series between the RCP8.5 and RCP8.5_FixA simulation scenarios further reveal that the future reduced aerosols emissions will contribute to strengthening the long-term correlation of precipitation records in Huai river basin in summer during the late-21st century (2071-2100) and the scaling exponents will increase by more than 0.1 in comparison with the present condition (1987-2016).

Keywords: precipitation; aerosols; detrended fluctuation analysis (DFA)

1 Introduction

As we all know, the weather changes with short-term correlation. This feature can be maintained for a week (the duration of a weather system) (Havlin et al., 1999). However, it is noteworthy that, in recent years, results of the nonlinear research have shown that changes in the climate system have self-memory. That is to say, the past climate evolution has a long-term effect on the future evolution of the climate system (Monetti et al., 2003). This effect is the so-called “long-term correlation”, “long-term memory” or “long-term persistence” in nonlinear science. Long-term correlation essentially describes the self-similarity of the evolution of climate system at different timescales. Therefore, climate variability characteristics on a large timescale can be inferred from the features of the climate system itself on a small timescale (Shukla, 1998). In fact, in early 1951, Hurst, a British hydrologist (Hurst, 1951), discovered that long-term correlation characteristics existed in nature when he studied the variation of water flow in the Nile. He found that if there is a large amount of water flowing in the first year, the river’s water flow of the following year would be larger, which showed that the system had a clear long-term correlation characteristic. With the unremitting research of scientists, long-term correlation characteristics have been found in many climate variables, such as precipitation series (Bunde et al., 2013; Zhao and He, 2015; Jiang et al., 2017), temperature records (Monetti et al., 2003; Király et al., 2005; Yuan et al., 2015), wind speed records (Koçak, 2009), ozone (Varotsos et al., 2006), and outgoing longwave radiation (Shen et al., 2017). People cannot accurately quantify the intensity of long-term correlation by the simple calculation of autocorrelation function and power spectral density due to the non-stationarity of time series (Talkner et al., 2000). In order to solve this problem, the detrended fluctuation analysis (DFA) technique was introduced and generalized by Peng et al. (1994) and Bunde et al. (2000). DFA can effectively filter out the strong trend components caused by external forcing in time series and excavate the fluctuation components induced by the long-term correlation. Due to its advantages and applicability (Bashan et al., 2008), in recent years, this method has been widely used to study the evolution of the climate system (Kantelhardt et al., 2006; Fraedrich et al., 2009; Zhu et al., 2010; Bunde et al., 2013; Jiang et al., 2015, 2017; Yuan et al., 2015; He et al., 2015) and to evaluate the performance of climate models (Govindan et al., 2002; Blender and Fraedrich, 2003; Zhao and He, 2015). Zhao and He (2015) evaluated the precipitation simulation skills of the BCC_CSM1.1 (m) by comparing the differences of the scaling exponents between the climate model-simulated and observational data. Jiang et al. (2017) investigated the scaling behaviors of precipitation over China and found that the precipitation time series in some stations exhibit long-term correlation and the scaling exponents are less than 0.62, showing weak correlation characteristics.

Recently, urban air pollution in China has become increasingly severe and the haze weather frequently occurs in major cities such as Beijing due to high pollutant emissions (Yin et al., 2015; Cai et al., 2017). Aerosols, as one of the significant components of pollutants, would be reduced in the future for their harmful effects on human health as well as the environment (Wang et al., 2017). Precipitation, as one of the most important climate variables, exerts a huge impact on agriculture, water resource management and human activities (Walther et al., 2002). At present, much effort has been made to detect and analyze the trend in the occurrence of extreme precipitation events under future reduced aerosols emissions. Wang et al. (2016) analyzed the effect of reduced aerosols emissions on projected extreme precipitation events and found that some extreme precipitation events would become more and more frequent in the future. However, the potential impacts of future reduced aerosols on internal dynamics characteristics of precipitation series have not been widely discussed before. Southern China, located in regions south of the Huai River and Qinling Mountains and east of the Qinghai-Tibet Plateau, is significantly affected by weather systems (e.g., subtropical high, southwest vortex) and climate factors (e.g., El Niño Southern Oscillation, Pacific Decadal Oscillation, Indian Ocean Dipole Mode and Atlantic Multi-decadal Oscillation) (Yang et al., 2004; Si and Ding, 2016; Zhu et al., 2016). Due to its complex climate characteristics, the prediction skill for short-term and long-term climate change is limited in southern China. In this paper, the DFA technique is used to analyze potential impacts of future reduced aerosols on internal dynamics characteristics of precipitation in southern China. Such a study may contribute to understanding the inherent precipitation evolution and further improve forecast skills in southern China.

This study is organized as follows. In Section 2, the source and details of data used in this paper are introduced and the calculation steps of the DFA technique are described. In Section 3, the scaling behaviors of precipitation in southern China are detected and the performance of Community Earth System Model (CESM1) is evaluated. In

Section 4, the potential impacts of reduced aerosols on internal dynamics characteristics of precipitation in southern China are investigated. The conclusion and possible mechanisms are given in Section 5.

2 Materials and Method

2.1 Data

The grid precipitation data with 0.5x0.5 horizontal resolution used to evaluate the performance of CESM1 climate model is selected from the National Meteorological Information Center of China (http://data.cma.cn/site/index.html). The data covers 11315 days from 1961 to 2007 (Xie et al., 2007). In this paper, we select the data from 1976 to 2005 as observations in order to keep the consistency of the output data period from a climate model. The global climate model (GCM) used in this paper is Community Earth System Model (CESM1), which is a fully coupled ocean-atmosphere-land-sea ice model and can simulate the Earth's climate states for the past, present and future (Hurrell et al., 2013). The simulation scenarios for the 21st century is documented in Meehl et al., (2013). The horizontal resolution is 0.9° latitude x 1.25° longitude for the atmosphere and land and 1° latitude x 1° longitude for the ocean. The CESM1 includes three-mode modal aerosols scheme (MAM3 scheme) that can simulate aerosols concentrations and internal mixtures for dust, organic carbons, sulfate, sea salt and black carbon (Liu et al., 2012). The daily precipitation data from CESM1 history simulation during 1976-2005 are used to evaluate the performance of CESM1. The daily precipitation data from the RCP8.5

Large Ensemble simulation (Kay et al., 2014) and RCP8.5 with fixed aerosols (RCP8.5_FixA) simulation (Xu et al., 2015; Wang et al., 2016) are used to study the potential impacts of reduced aerosols on internal dynamics characteristics of precipitation. The RCP8.5 simulation scenario assumes that the energy demand and greenhouse gas (GHG) emissions are comparatively high in the future due to the imbalance between the rapidly increasing population and relatively slow technological innovation and improvements of energy structure. It includes 30 ensemble members forced by the same trajectory of aerosols emissions and the equivalent GHG but starts from a different atmospheric initial condition (1920-2100). The RCP8.5_FixA (15 members) simulation scenario uses the same forcing as the RCP8.5 simulation scenario except that all aerosols emissions and tropospheric oxidants are fixed at 2005 levels. The variation of internal dynamics characteristics of precipitation is examined during the late-21st century (2071-2100) in comparison with the present condition (1987-2016) under the climate scenario RCP8.5 and RCP8.5_FixA. Therefore, the results are compared to assess the effect of reduced aerosols emissions on internal dynamics characteristics of precipitation under the different RCP8.5 simulation scenarios.

2.2 The DFA method

Recently, more and more scientists are beginning to focus on the non-stationary characteristics of climate series. Many different analysis techniques, such as the rescaled range (R/S) analysis technique (Hurst et al., 1951), the fluctuation analysis technique (Peng et al., 1992), the detrending moving average analysis technique

(Alessio et al., 2002) and the detrended fluctuation analysis technique (Peng et al., 1994), have been proposed. DFA was proposed by Peng et al. (1994) to detect the long-term correlation in climate time series. The more detailed introduction is documented in Bunde et al. (2000) and Kantelhardt et al. (2001). Here, a brief introduction about the generalized DFA technique is summarized as follows.

The precipitation time series $\{x(i), i=1,2,\cdots\cdots N\}$ with annual cycle removed is considered and its cumulative sum, which is better known as the profile, is defined as

$$y(j)=\sum_{i=1}^{i=j}\Delta x(i) \qquad (j=1,2,\cdots\cdots N).$$

Then, the profile $y(j)$ is divided by m non-overlapping segments of size s. In order to make full use of the remaining data, we can obtain $2m$ segments by redividing the profile from its back to front. In each segment, the local trend $p(v,j)$ is calculated by least squares fit (n-order DFA corresponding n-order polynomial) and the residuals are obtained as

$$Q(v,j)=y(v,j)-p(v,j) \qquad (v=1,2,\cdots\cdots 2m; j=1,2,\cdots\cdots,s) .$$

The variance for each segment is defined as

$$H(v,s)=\frac{1}{s}\sum_{j=1}^{s}Q^2(v,j) \qquad (v=1,2,\cdots\cdots,2m).$$

Finally, the fluctuation function can be obtained by the arithmetic mean of the fluctuation function in all the segments

$$F(s)=\left[\frac{1}{2m}\sum_{v=1}^{2m}H(v,s)\right]^{1/2}.$$

For long-term corrected time series, the fluctuation function and timescale s exhibit that the power law relationship $F(s)\sim s^{\alpha}$ and $F(s)$ will increase with the timescale s. α represents the scaling exponent of time series. If $0.5<\alpha<1$

($0 < \alpha < 0.5$), the time series exhibit a positive (negative) long-term correlation characteristics. If α=0.5, the time series are uncorrelated. In this paper, the second-order DFA (DFA2) technique is adopted, which has been commonly employed to study the long-term memory characteristics of climate variability (Zhao and He, 2015; He et al., 2015; Shen et al., 2017).

2.3 Uncertainties in the DFA results

The long-term memory characteristics of a given climate variable can be quantitatively described by using the DFA method. However, there are some uncertainties due to the length of the observed data. Therefore, the uncertainties should be estimated with the quantitative analysis of the long-term memory characteristics of precipitation series over southern China. Because the scaling exponent of precipitation series is between 0.5 and 0.7, the uncertainty of α=0.5, α=0.6 and α=0.7 are examined as follows. Each test produces 20000 artificial series (10000 artificial series for daily precipitation and another 10000 artificial series for seasonal precipitation) with the given scaling exponents (α=0.5; α=0.6; α=0.7) by Fourier filtering (Peng et al., 1991; Lennartz and Bunde et al., 2011), and the length of the artificial series is the same as that of the precipitation series over southern China used in this study. By using the DFA, scaling exponents of the artificial series are shown in Figure 1. For α=0.5, 99% of the scaling exponents are between 0.46 and 0.54 as 0.5% to 99.5% range; the result of scaling exponents has a deviation ranging from -0.04 to 0.04 in the confidence interval of 99%. For α=0.6, 99% of the scaling exponents are between 0.56 and 0.65 as 0.5% to 99.5% range; that is to say, the result of scaling exponents has a deviation ranging from -0.04 to 0.05 in the confidence interval of 99%. For α=0.7, 99% of the scaling exponents are between 0.65 and 0.75 as 0.5% to 99.5% range, indicating that the result of scaling exponents has a deviation ranging from -0.05 to 0.05 in the confidence interval of 99%. According to the above discussions, we define the variation ranging from -0.05 to 0.05 as the 0.01 significant test level of precipitation series over southern China.

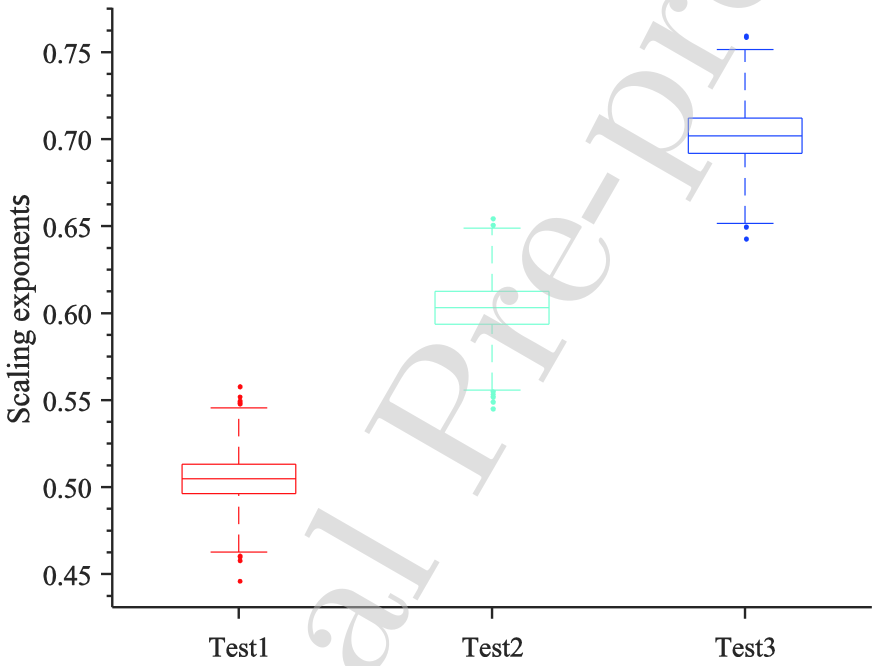

Figure.1 The DFA analysis of the artificial series generated with given scaling exponents by Fourier filtering.

3 Results

3.1 Scaling behaviors of precipitation series

The temporal evolution and profile of regional average precipitation time series over southern China during 1976-2005 are shown in Figure 2a and 2b, respectively. We notice that the precipitation anomaly series exhibit irregular high-frequency fluctuations and their profiles show the inter-annual oscillation. The double logarithmic curve of the fluctuation function F(s) with timescales is shown in Figure 2c for the time series of regional average precipitations over southern China. By linear fitting, it is seen that the precipitation time series (regional average) over southern China exhibit relatively weak long-term correlation characteristics with scaling exponents of 0.61. Moreover, the scaling exponent of randomly shuffled precipitation records is 0.5 with white noise characteristics, which further verifies the fact that the long-term correlation characteristics of precipitation series over southern China are caused by the fractal characteristics.

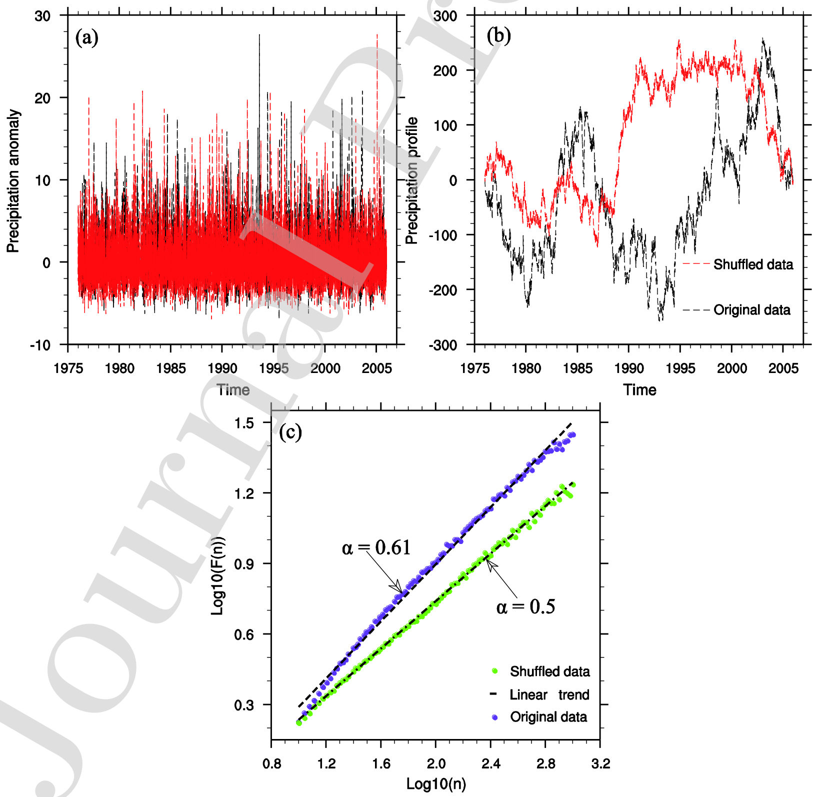

Figure.2 (a) The regional mean precipitation anomaly time series over southern China (the black dashed line represents raw precipitation time series and the red dashed line represents randomly shuffled precipitation time series). **(b)** The cumulative deviation for raw (black dashed line) and randomly shuffled (red dashed line) precipitation time series over southern China. **(c)** The DFA analysis results for annual precipitation time series (regional mean) over southern China from 1976 to 2005 (the purple (raw time series) and green (randomly shuffled time series) solid point represent the obtained fluctuation function; the black dashed line represents the linear fitting line of the red solid point, and the slope can be a good index for long-term memory characteristics on this timescale).

The scaling analysis of precipitation series (regional average) over southern China in four seasons is shown in Figure 3 to further investigate whether daily precipitation data has long-term correlation characteristics in all four seasons. The scaling exponents for precipitation series in the four seasons are 0.52, 0.58, 0.64 and 0.67, respectively. The more obvious long-term correlation characteristics are shown in autumn and winter, while the scaling exponents are close to 0.5 in spring and summer suggesting the uncorrelation. Figure 4 shows the spatial distribution of scaling exponents of the precipitation series over southern China. It is seen that the scaling exponents of annual precipitation records show a decreasing trend from the coast to the inland over southern China. The scaling exponents in the coastal areas, Guangdong, southern Anhui and southeastern Jiangxi provinces in particular, are close to 0.6 showing strong long-term correlation, while they are close to 0.5 showing the uncorrelation in inland areas, Chongqing and western Hubei province in particular.

The distribution feature for scaling exponents of precipitation series is closely related to the climatic conditions in the region. The precipitation in coastal areas is mainly affected by weather systems (e.g., subtropical high, southwest vortex) and climate factors (e.g., El Niño Southern Oscillation, Pacific Decadal Oscillation, Indian Ocean Dipole Mode and Atlantic Multi-decadal Oscillation), while precipitation in inland areas is mainly attributed to the re-evaporation of surface water, which is produced by the inland circulation system. The precipitation affected by weather systems is more organized. Hence it presents stronger long-term correlation. However, the precipitation produced by the inland circulation system is more random, so that it shows the less correlation. In spring, the scaling exponents of precipitation sequence are ranged from 0.48 to 0.52 in most areas of southern China, showing the uncorrelation. The regions with the scaling exponents between 0.58 and 0.62 are mainly located in Guangdong, Zhejiang, northwestern Anhui and southeastern Henan provinces indicating that the precipitation records exhibit positive long-term correlation in these regions. However, the scaling exponents are smaller than 0.46 in the northeastern Chongqing and southwestern Hubei province showing weak negative long-term correlation. In summer, the precipitation records exhibit obvious positive long-term correlation with the scaling exponents greater than 0.62 in the downstream areas of the Yangtze River. At the same time, the scaling exponents are close to 0.5 showing the uncorrelation in most of the other southern China regions. In autumn, the precipitation records exhibit relatively weak long-term correlation with the scaling exponents greater than 0.55 in most of the southern China regions. And the regions showing strong long-term correlation located in the southeastern Guangxi, southern Hunan and central Jiangxi provinces. In winter, the scaling exponents of precipitation records are significantly greater than 0.66 exhibiting strong long-term correlation in the provinces of Henan, southern Zhejiang, Fujian, Guangdong and Jiangxi, and especially high in Guangdong province.

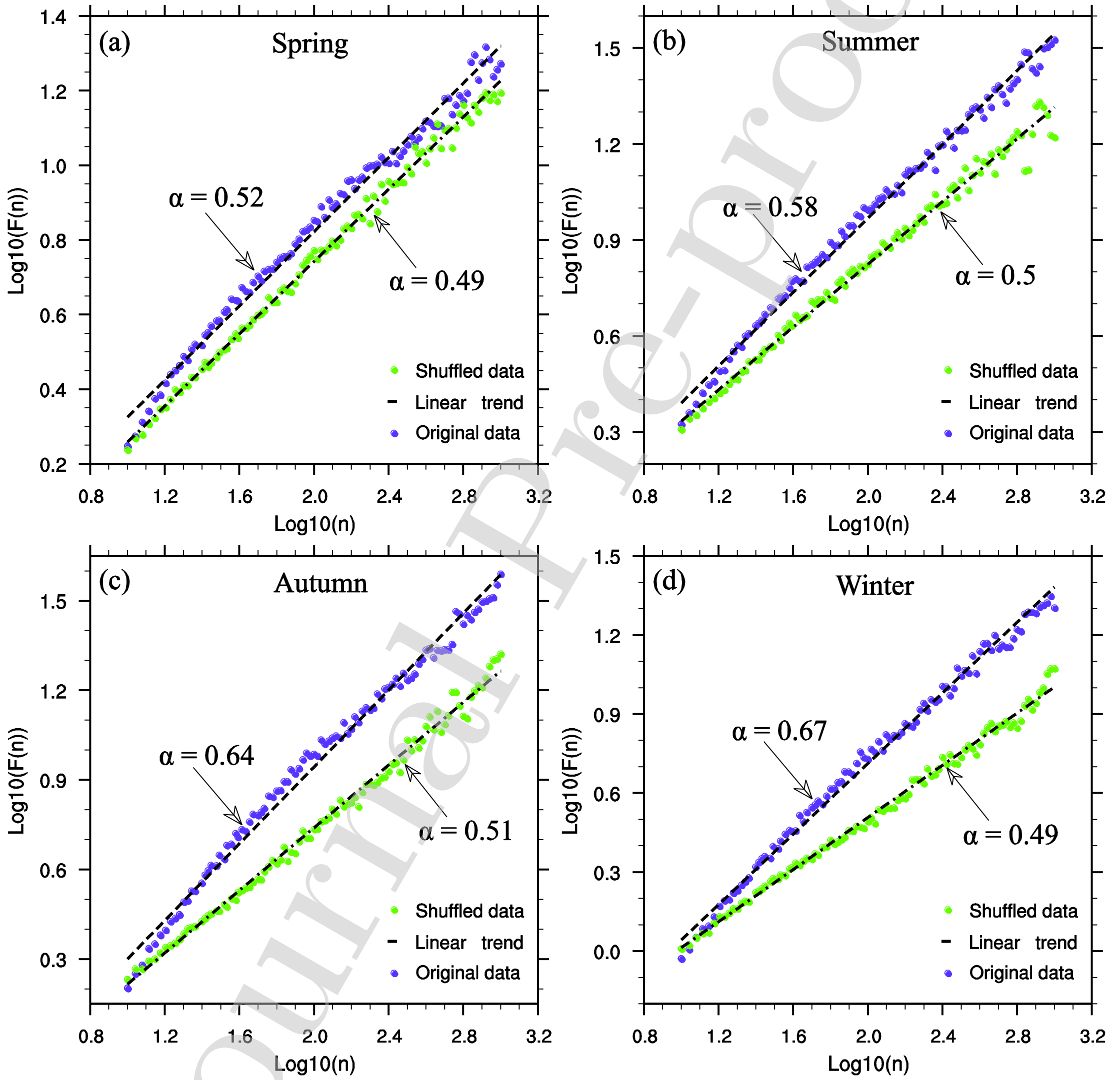

Figure.3 The DFA analysis result for four seasons time series (regional mean) over southern China from 1976 to 2005 (the purple (raw time series) and green (randomly shuffled time series) solid point represent the obtained fluctuation function; the black dashed line represents the linear fitting line of the red solid point, and the slope can be

a good index for long-term memory characteristics on this timescale); (a) Spring; (b) Summer; (c) Autumn; (d) Winter.

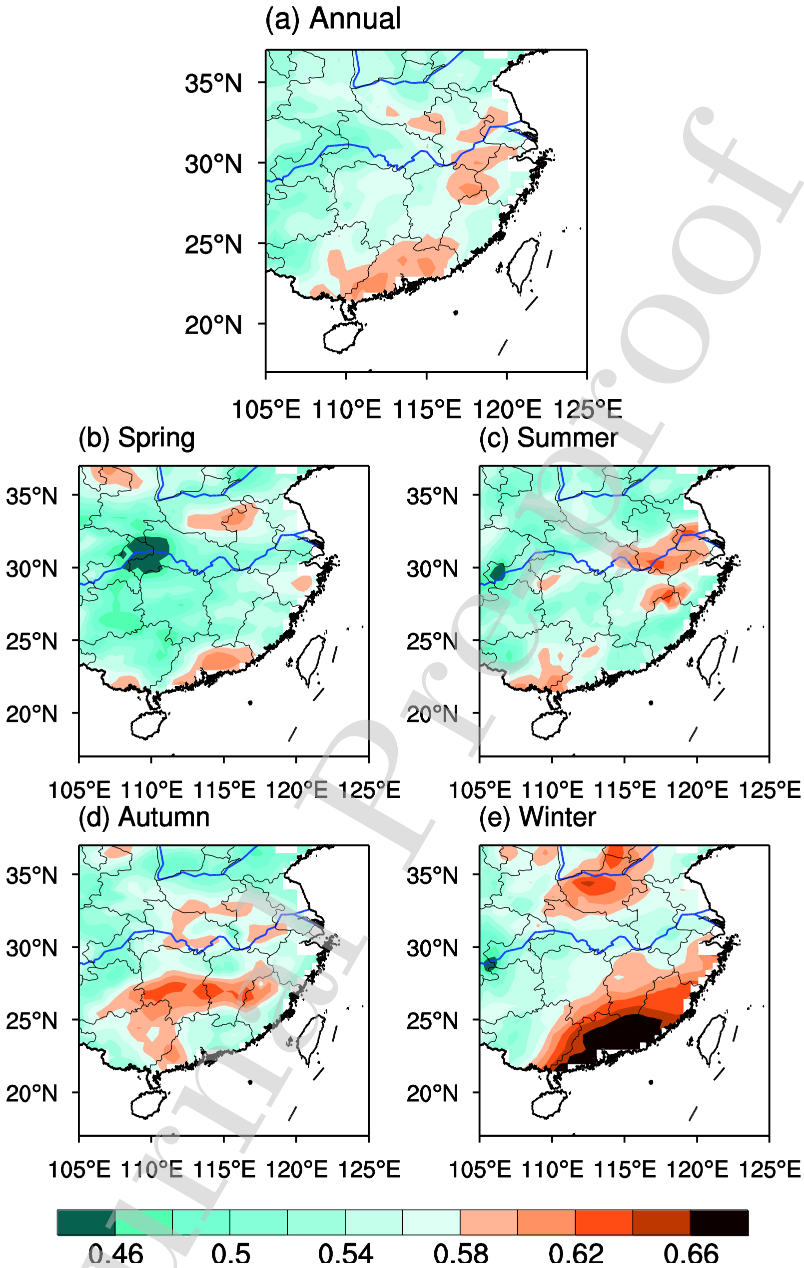

Figure.4 The spatial pattern of scaling exponents for precipitation records from 1976 to 2005 over southern China in annual and four seasons. (a) Annual; (b) Spring; (c) Summer; (d) Autumn; (e) Winter.

3.2 Evaluation of the performance of CESM1

Although the performance of CESM1 to simulate precipitations in China have been evaluated (Wang et al., 2017), the differences of scaling exponents of precipitation records between observations and simulations are shown in Figure 5 to evaluate the performance of CESM1 in simulating the internal dynamics characteristics of precipitation over southern China. Compared with the observation, the simulated scaling exponents of annual precipitation records are close to observation in most of southern China regions, and only 9% of grid points pass the 99% errors significance test. However, in places like Guizhou, Fujian and western Guangxi provinces the simulated scaling exponents are apparently overvalued. As for the seasonal evaluations, the simulated scaling exponents of precipitation records in spring are larger in eastern Guangxi province and smaller in northwestern Anhui and central Henan provinces than the observed ones. In summer, the simulated results are significantly greater than observations in Guangdong and Fujian provinces with errors more than 0.1. When it comes to autumn, Guizhou, Chongqing, northeastern Guangdong, southern Shanxi and southern Shandong are regions with distinguishably higher simulated values. While in winter, the simulated scaling exponents are almost consistent with the observations in most of southern China regions and only 9% of grid points pass the 99% errors confidence test. Overall, there are 90%, 79%, 72% and 91% of grid points display the almost identical scaling exponents with the observed scaling exponents in spring, summer, autumn and winter, respectively, indicating that the CESM1 has the ability to simulate the internal dynamics characteristics of precipitation series in southern China.

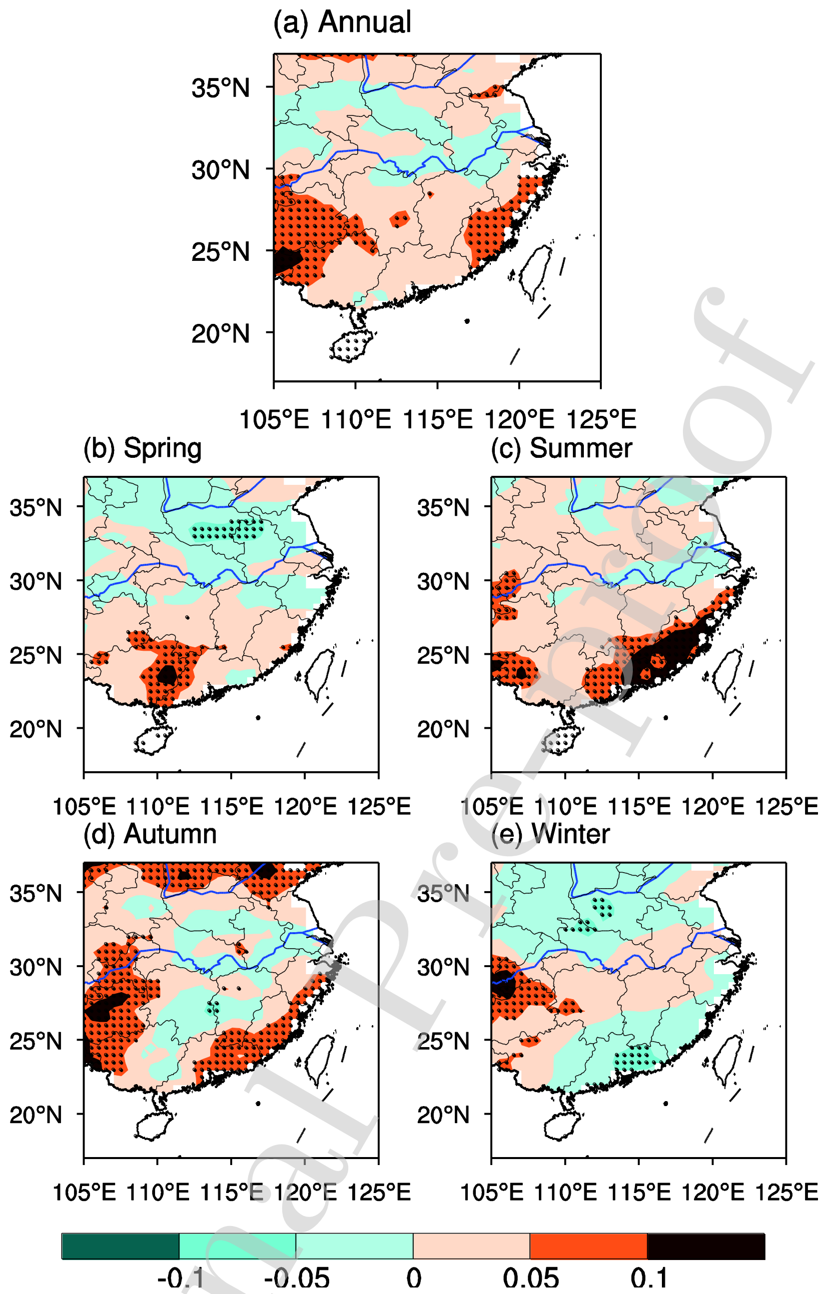

Figure.5 The spatial pattern of the differences for scaling exponents between observations and CESM1 simulated precipitation records from 1976 to 2005 over southern China in annual and four seasons. (a) Annual; (b) Spring; (c) Summer; (d) Autumn; (e) Winter (The black dots indicate that the differences of scaling exponents between observation and simulation results pass the 99% significance test).

3.3 The impacts of future reduced aerosols on internal dynamics characteristics

of precipitation series

Figure 6 shows the spatial pattern of changes in scaling exponents of annual precipitation series over southern China during the late-21st century (2071-2100) under the RCP8.5 and RCP8.5_FixA simulation scenarios in comparison with the present condition (1987-2016). It can be seen that the long-term correlation of precipitation records in Huai river basin will increase in values during the late-21st century (2071-2100) under the RCP8.5 simulation scenario (Figure 6b). However, the long-term correlation of precipitation records over all southern China regions are consistent with present condition (1987-2016) during the late-21st century (2071-2100) under the RCP8.5_FixA simulation scenario (Figure 6c). Based on the differences between the RCP8.5 and RCP8.5_FixA simulation scenarios (Figure 6d), we found that the future reduced aerosols will significantly strengthen the long-term correlation characteristics of precipitation records in Huai river basin.

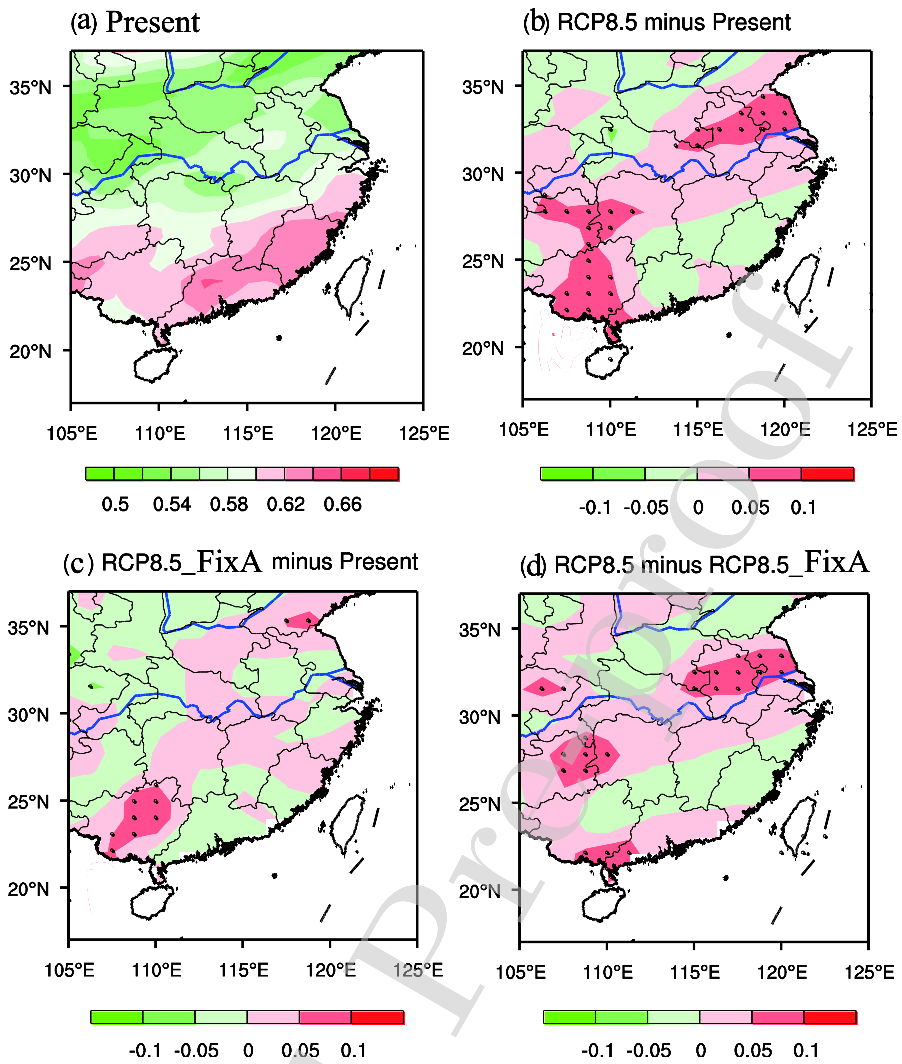

Figure.6 The spatial pattern of changes in scaling exponents of annual precipitation series over southern China during the late-21st century (2071-2100) under the RCP8.5 and RCP8.5_FixA scenarios in comparison with the present condition (1987-2016). (a) The scaling exponents of the present condition (1987-2016); (b) the differences of scaling exponents between the RCP8.5 and present scenarios; (c) the differences of scaling exponents between the RCP8.5_FixA and present scenarios; (d) the differences of scaling exponents between the RCP8.5 and RCP8.5_FixA scenarios. The black dots indicate that the differences of scaling exponents between the two scenarios pass the 99% significance test.

Figure 7 presents the variation characteristics of scaling exponents of precipitation series in the four seasons by using the DFA technique. In spring, the distribution of variations on scaling exponents is complicated in southern China during the late-21st century (2071-2100) under the RCP8.5 simulation scenario (Figure 7b). The significant change mainly occurs in the south of the Yangtze River. Augmentation of the long-term correlation can be found in Guangxi, northeastern Guizhou, northwestern Hunan, northern Jiangxi and Ningxia provinces while in Fujian and central Jiangxi provinces the long-term correlation declines. Under the RCP8.5_FixA simulation scenario (Figure 7c)， An obvious seesaw between the south and north of the Yangtze River can be observed in the long-term correlation of precipitation records, with distinct intensification in the north and reduction in the south. Figure 7d shows the differences of scaling exponents calculated by precipitation series between the RCP8.5 and RCP8.5_FixA simulation scenarios. It indicates that the future reduced aerosols emissions will weaken the long-term correlation of precipitations in the north of the Yangtze River but strengthen the long-term correlation of precipitations in the most of southern Yangtze River regions, Guangdong and Guangxi provinces in particular. In summer, regions with the obvious change of scaling exponents of precipitation series located in Huai river basin and the scaling exponents will increase during the late-21st century (2071-2100) under the RCP8.5 simulation scenario in comparison with the present condition (1987-2016) (Figure 7f). Meanwhile, there is a noticeable decrease in the long-term correlation of precipitation records in a few areas (Guizhou and Guangdong provinces) both under the RCP8.5

(Figure 7f) and RCP8.5_FixA simulation scenario (Figure 7g). By analyzing the differences of scaling exponents of precipitation series between the RCP8.5 and RCP8.5_FixA simulation scenarios (Figure 7h), we can find that the future reduced aerosols emissions will contribute to reinforcing the long-term correlation of precipitation records in Huai river basin in summer since the scaling exponents increase by more than 0.1. In autumn, the long-term correlation of precipitation records will decrease in the north of the Yangtze River and slightly increase in the south under the RCP8.5 simulation scenario (Figure 7i). When it comes to the RCP8.5_FixA simulation scenario (Figure 7k), more regions present the reduced long-term correlation during the late-21st century (2071-2100) in comparison with the present condition (1987-2016). Therefore, the future reduced aerosols emissions may result in reinforcing of the long-term correlation of precipitation records in southern Hunan and southwestern Jiangxi provinces and diminishing the long-term correlation of precipitation records in the north of Hubei and the south of Henan provinces (Figure 7l). In winter, the long-term correlation of precipitation records will increase in most regions of southern China under the RCP8.5 and RCP8.5_FixA simulation scenarios during the late-21st century (2071-2100) in comparison with the present condition (1987-2016), especially in Guangxi, Guangdong and Fujian provinces under the RCP8.5 simulation scenario and in Huai river basin under the RCP8.5_FixA simulation scenario (Figure 7n and 7o). The differences of scaling exponents of precipitation series between the RCP8.5 and RCP8.5_FixA simulation scenarios in winter are less distinct as other seasons, suggesting the future reduced aerosols emissions will generate less effect on the internal dynamics characteristics of precipitation series in winter over southern China (Figure 7p).

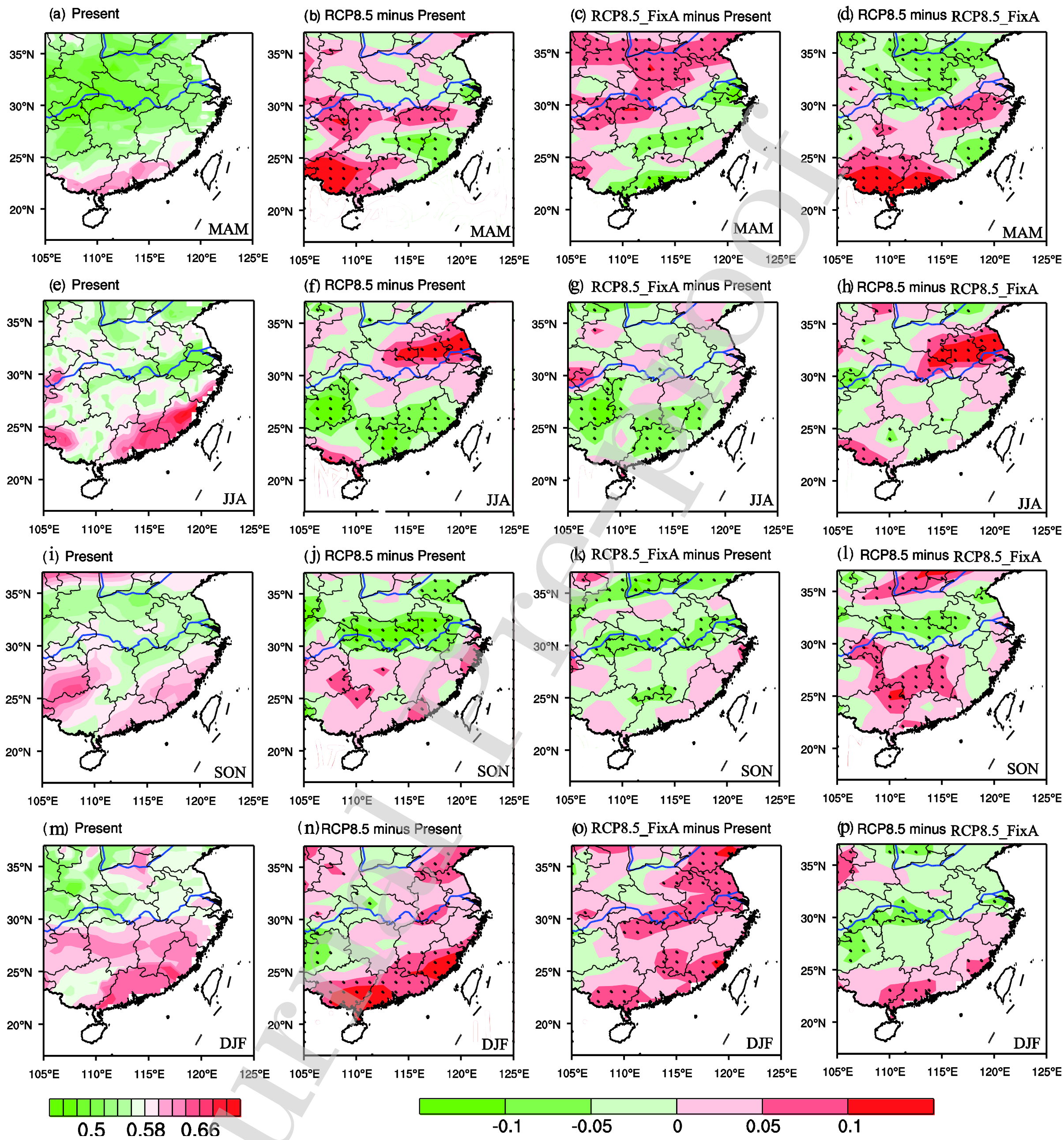

Figure.7 Same as the **Figure.6** but for four seasons. (a-d) Spring; (e-h) Summer; (i-l) Autumn; (m-p) Winter.

4 Conclusion and possible mechanisms

In this study, the scaling behaviors of precipitation records over southern China are investigated by using the DFA method. It is found that the precipitation records over southern China exhibit relatively weak long-term correlation characteristics. The scaling exponents in coastal areas are close to 0.6 showing long-term correlation but the values in inland areas are close to 0.5 showing the uncorrelation. The shuffled precipitation time series is analyzed by the DFA technique to further verify the fact that the long-term correlation characteristics for precipitation series over southern China are caused by fractal characteristics. Based on the long-term correlation characteristics of the observed precipitation records, the performance of CESM1 in simulating precipitations over southern China is evaluated. The simulation results show that 90%, 79%, 72%, and 91% of grid points for precipitation records over southern China are close to observation results in the four seasons, respectively, which indicate that the CESM1 have the ability to simulate the internal dynamics characteristics of precipitation series in southern China. Based on simulated precipitation data by CESM1, the changes of scaling exponents of precipitation series over southern China are investigated during the late-21st century (2071-2100) in comparison with the present condition (1987-2016) under the climate scenarios RCP8.5 and RCP8.5_FixA. Then the differences between the climate scenarios RCP8.5 and RCP8.5_FixA are analyzed to assess the contribution of future reduced aerosols emissions on the internal dynamics characteristics of precipitation. It is found that there are obvious changes of internal dynamics characteristics of precipitation records over southern China during the late-21st century (2071-2100) under both the RCP8.5 and RCP8.5_FixA simulation scenarios in comparison with the present condition (1987-2016) in summer. During the late-21st century (2071-2100)，the long-term correlation for precipitation will be intensified in Huai river basin under the RCP8.5 simulation scenario. Meanwhile, there is noticeable decrease in the long-term correlation of precipitation records in a few areas (Guizhou and Guangdong provinces) both under the RCP8.5 (Figure 7f) and RCP8.5_FixA simulation scenario (Figure 7g). And the differences of scaling exponents of precipitation series between the RCP8.5 and RCP8.5_FixA simulation scenarios further indicate that the future reduced aerosols emissions will contribute to strengthening the long-term correlation of precipitation records in Huai river basin in summer with an increment of more than 0.1 in the scaling exponents during the late-21st century (2071-2100) in comparison with the present condition (1987-2016).

The present paper demonstrated the fact that the future reduced aerosols emissions will contribute to strengthening the long-term correlation of precipitation records in Huai river basin in summer during the late-21st century (2071-2100) in comparison with the present condition (1987-2016). But the possible mechanisms of how the future reduced aerosols emissions manage to induce the long-term correlation of precipitation records to strengthen in Huai river basin in summer require further investigations and discussions. Previous studies have proposed that aerosols have a significant impact on precipitation through multiple processes. (i) Aerosols can directly change the energy of solar radiation reaching the land surface through its own optical properties. (ii) Aerosols have important microphysical effects on clouds and precipitation through their influence on cloud drop nucleation, which can influence cloud lifetime, cloud albedo, and precipitation (Ramaswamy et al., 2001; Qian et al., 2009). (iii) Aerosols indirectly influence the precipitation through affecting the strength of the East Asian summer monsoon (Xie et al., 2016), weather systems (e.g., subtropical high, southwest vortex) and climate factors (e.g., El Niño Southern Oscillation, Indian Ocean Dipole Mode and North Atlantic Oscillation). Figure 8 shows the anomalies of temperature and 850hPa horizontal wind under the RCP8.5 and RCP8.5_FixA scenarios from 2071 to 2100 in southern China. The reduction of aerosols will increase the amount of solar radiation that reaches the land surface, which results in the strong positive temperature anomalies (~1.4 ℃) in Huai river basin in summer. Therefore, more heat is available for evaporating water and energizing convective rain clouds. Meanwhile, more warming of the air above the surface can destabilize the low atmosphere and promote the generation of convective clouds. On the other hand, fewer aerosols mean relatively less cloud condensation nuclei (CCN), which is expected to speed up the conversion of cloud water into smaller raindrops and increase the precipitation from shallow and short-lived clouds. In addition, there is an anomalous cyclonic circulation over Huai river basin, which is favorable for wind convergence at the low troposphere (850hPa). The anomalous vertical upward movement combined with sufficient moisture can lead to more precipitation in Huai river basin. In summer, there is a large amount of precipitation in Huai river basin due to more favorable background conditions. Moreover, the anomalous precipitation brought by the future reduced aerosols emissions can further increase the intensity and duration of precipitation, which is beneficial to intensify the correlation among precipitations in Huai river basin. To some extent, it can explain the fact that the future reduced aerosols emissions will contribute to strengthening the long-term correlation of precipitation records in Huai river basin in summer during the late-21st century (2071-2100) in comparison with the present condition (1987-2016). Although the current knowledge about the effects of aerosols on precipitations has made great progress, it is still very limited. Thus, more physical mechanisms of the impact of aerosols on internal dynamics characteristics of precipitation need to be further investigated in the future.

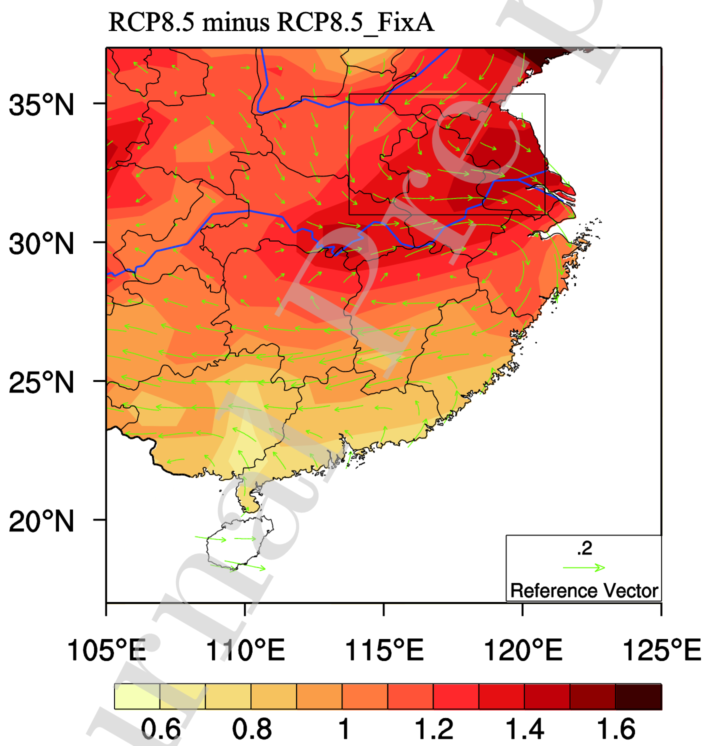

Figure.8 The climatic averaged differences of temperature (shading in °C) and 850hPa horizontal wind (vector in m/s) between the RCP8.5 and RCP8.5_FixA scenarios from 2071 to 2100 over southern China. The changes are significant based on a two sample student's test at the 95% confidence intervals.

Finally, it should be pointed out that long-term correlation is quite common in the climate system. The increase of scaling exponents of precipitation records in Huai river basin in summer indicates that cumulative historical effects on current precipitation state will become stronger with reduced aerosols emissions in the future, which is significant to further improve forecasting skills of precipitations in Huai river basin.

Acknowledgments

The work was supported by the National Natural Science Foundation of China (41675003 and 41675056). Any conflicts of interest for any author that are not apparent from their affiliations or funding. The data used in this study can be acquired from the National Meteorological Information Center of China (http://data.cma.cn/site/index.html) and the Climate data Gateway at NCAR (https://www.earthsystemgrid.org/dataset/ucar.cgd.ccsm4.output.html).

Reference

Alessio E, Carbone A, Castelli G, et al. Second-order moving average and scaling of stochastic time series[J]. The European Physical Journal B-Condensed Matter and Complex Systems, 2002, 27(2): 197-200.

Bashan A, Bartsch R, Kantelhardt J W, et al. Comparison of detrending methods for fluctuation analysis[J]. Physica A: Statistical Mechanics and its Applications, 2008, 387(21): 5080-5090.

Bunde A, Büntgen U, Ludescher J, et al. Is there correlation in precipitation?[J]. Nature climate change, 2013, 3(3): 174-175.

Bunde A, Havlin S, Kantelhardt J W, et al. Correlated and uncorrelated regions in heart-rate fluctuations during sleep[J]. Physical Review Letters, 2000, 85(17): 3736.

Blender R, Fraedrich K. Long time correlation in global warming simulations[J]. Geophysical Research Letters, 2003, 30(14).

Cai W, Li K, Liao H, et al. Weather conditions conducive to Beijing severe haze more frequent under climate change[J]. Nature Climate Change, 2017, 7(4): 257-262.

Fraedrich K, Blender R, Zhu X. Continuum climate variability: Long-term correlation, scaling, and 1/f-noise[J]. International Journal of Modern Physics B, 2009, 23(28n29): 5403-5416.

Govindan R B, Vyushin D, Bunde A, et al. Global climate models violate scaling of the observed atmospheric variability[J]. Physical Review Letters, 2002, 89(2):

028501.

Havlin S, Buldyrev S V, Bunde A, et al. Scaling in nature: from DNA through heartbeats to weather[J]. Physica A: Statistical Mechanics and its Applications, 1999, 273(1): 46-69.

He W, Zhao S, Liu Q, et al. Long-term correlation in the drought and flood index from 1470 to 2000 in eastern China[J]. International Journal of Climatology, 2015.

Hurrell J W, Holland M M, Gent P R, et al. The community earth system model: a framework for collaborative research[J]. Bulletin of the American Meteorological Society, 2013, 94(9): 1339-1360.

Hurst H E. Long-term storage capacity of reservoirs[J]. Trans. Amer. Soc. Civil Eng., 1951, 116: 770-808.

Jiang L, Li N, Fu Z, et al. Long-term correlation behaviors for the 0-cm average ground surface temperature and average air temperature over China[J]. Theoretical and Applied Climatology, 2017, 119(1-2): 25-31.

Jiang L, Li N, Zhao X. Scaling behaviors of precipitation over China[J]. Theoretical and Applied Climatology, 2015: 1-8.

Kantelhardt J W, Koscielny-Bunde E, Rybski D, et al. Long-term persistence and multifractality of precipitation and river runoff records[J]. Journal of Geophysical Research: Atmospheres, 2006, 111(D1).

Kay J E, Deser C, Phillips A, et al. The Community Earth System Model (CESM) large ensemble project: A community resource for studying climate change in the presence of internal climate variability[J]. Bulletin of the American Meteorological Society, 2015, 96(8): 1333-1349.

Király A, Jánosi I M. Detrended fluctuation analysis of daily temperature records: Geographic dependence over Australia[J]. Meteorology and Atmospheric Physics, 2005, 88(3): 119-128.

Koçak K. Examination of persistence properties of wind speed records using detrended fluctuation analysis[J]. Energy, 2009, 34(11): 1980-1985.

Lennartz S, Bunde A. Distribution of natural trends in long-term correlated records: A scaling approach[J]. Physical Review E, 2011, 84(2): 021129.

Liu X, Easter R C, Ghan S J, et al. Toward a minimal representation of aerosols in climate models: Description and evaluation in the Community Atmosphere Model CAM5[J]. Geoscientific Model Development, 2012, 5(3): 709.

Monetti R A, Havlin S, Bunde A. Long-term persistence in the sea surface temperature fluctuations[J]. Physica A: Statistical Mechanics and its Applications, 2003, 320: 581-589.

Meehl G A, Hu A, Arblaster J M, et al. Externally forced and internally generated decadal climate variability associated with the Interdecadal Pacific Oscillation[J]. Journal of Climate, 2013, 26(18): 7298-7310.

Peng C K, Havlin S, Schwartz M, et al. Directed-polymer and ballistic-deposition growth with correlated noise[J]. Physical Review A, 1991, 44(4): R2239.

Peng C K, Buldyrev S V. Long-range correlations in nucleotide sequences[J]. Nature, 1992, 356(6365): 168.

Peng C K, Buldyrev S V, Havlin S, et al. Mosaic organization of DNA nucleotides[J]. Physical review e, 1994, 49(2): 1685.

Qian Y, Gong D, Fan J, et al. Heavy pollution suppresses light rain in China: Observations and modeling[J]. Journal of Geophysical Research: Atmospheres, 2009, 114(D7).

Ramaswamy V, Boucher O, Haigh J, et al. Radiative forcing of climate change. In 'Climate change 2001: the scientific basis: contribution of working group I to the third assessment report of the Intergovernmental Panel on Climate Change'.(Eds J Houghton, Y Ding, D Griggs, M Noguer, P Van der Linden, X Dai, K Maskell, C Johnson) pp. 349–416[J]. 2001.

Shen Z, Shi J, Lei Y. Comparison of the Long-Range Climate Memory in Outgoing Longwave Radiation over the Tibetan Plateau and the Indian Monsoon Region[J]. Advances in Meteorology, 2017, 2017.

Shukla J. Predictability in the midst of chaos: A scientific basis for climate forecasting[J]. science, 1998, 282(5389): 728-731.

Si D, Ding Y. Oceanic forcings of the interdecadal variability in East Asian summer rainfall[J]. Journal of Climate, 2016, 29(21): 7633-7649.

Talkner P, Weber R O. Power spectrum and detrended fluctuation analysis: Application to daily temperatures[J]. Physical Review E, 2000, 62(1): 150.

Varotsos C, Kirk-Davidoff D. Long-memory processes in ozone and temperature variations at the region 60 S–60 N[J]. Atmospheric Chemistry and Physics, 2006, 6(12): 4093-4100.

Walther G R, Post E, Convey P, et al. Ecological responses to recent climate change[J]. Nature, 2002, 416(6879): 389-395.

Wang Z, Lin L, Yang M, et al. The effect of future reduction in aerosol emissions on climate extremes in China[J]. Climate dynamics, 2016, 47(9-10): 2885-2899.

Wang Z, Lin L, Zhang X, et al. Scenario dependence of future changes in climate extremes under 1.5° C and 2° C global warming[J]. Scientific Reports, 2017, 7.

Xie P, Chen M, Yang S, et al. A gauge-based analysis of daily precipitation over East Asia[J]. Journal of Hydrometeorology, 2007, 8(3): 607-626.

Xie X, Wang H, Liu X, et al. Distinct effects of anthropogenic aerosols on the East Asian summer monsoon between multidecadal strong and weak monsoon stages[J]. Journal of Geophysical Research: Atmospheres, 2016, 121(12): 7026-7040.

Xu Y, Lamarque J F, Sanderson B M. The importance of aerosol scenarios in projections of future heat extremes[J]. Climatic Change, 2015: 1-14.

Yang F, Lau K M. Trend and variability of China precipitation in spring and summer: linkage to sea‐surface temperatures[J]. International journal of climatology, 2004, 24(13): 1625-1644.

Yuan N, Fu Z, Liu S. Long‐term memory in climate variability: A new look based on fractional integral techniques[J]. Journal of Geophysical Research: Atmospheres, 2013, 118(23).

Yuan N, Fu Z, Liu S. Extracting climate memory using Fractional Integrated Statistical Model: A new perspective on climate prediction[J]. Scientific reports, 2014, 4.

Yuan N, Ding M, Huang Y, et al. On the long-term climate correlation in the surface air temperature records over Antarctica: A nonnegligible factor for trend evaluation[J]. Journal of Climate, 2015, 28(15): 5922-5934.

Yin Z, Wang H. The relationship between the subtropical Western Pacific SST and haze over North‐Central North China Plain[J]. International Journal of Climatology, 2016, 36(10): 3479-3491.

Zhao S, He W. Evaluation of the performance of the Beijing Climate Centre Climate System Model 1.1(m) to simulate precipitation across China based on long‐range correlation characteristics[J]. Journal of Geophysical Research Atmospheres, 2015, 120(24): 12576-12588.

Zhu X, Fraedrich K, Liu Z, et al. A demonstration of long-term correlation and climate predictability[J]. Journal of Climate, 2010, 23(18): 5021-5029.

Zhu Y, Wang T, Ma J. Influence of internal decadal variability on the summer rainfall in Eastern China as simulated by CCSM4[J]. Advances in Atmospheric Sciences, 2016, 33(6): 706.

*Declaration of Interest Statement

Declaration of interests

The authors declare that they have no known competing financial interests or personal relationships that could have appeared to influence the work reported in this paper.